



# Chapter 104

## Characteristic of Permeability and Porosity of a 2D High-Permeable Model with Etched Network Channels

Yanchao Fang<sup>1</sup>, Caili Dai<sup>1(✉)</sup>, Yongpeng Sun<sup>1</sup>, Ang Chen<sup>2</sup>,  
Yuanyin Wang<sup>1</sup>, and Lesley Anne James<sup>3</sup>

<sup>1</sup> School of Petroleum Engineering, China University of Petroleum (East China),  
Beijing, China

yczfang@163.com, {daic1, sunyongpeng}@upc.edu.cn

<sup>2</sup> Engineering Research Institute of Xinjiang Oil Field, Kelamayi, Xinjiang,  
China

<sup>3</sup> Faculty of Engineering and Applied Science, Memorial University of  
Newfoundland, St. John's, Newfoundland and Labrador, Canada

### 104.1 Introduction

In the process of oil production, waterflooding [4] is the most common development method for secondary production. However, long-term water injection could result in the formation of high-permeable zone in reservoir. The high-permeable zone would reduce water sweeping efficiency, making water injection ineffective.

To characterize the high-permeable zone, permeability and porosity are the two crucial parameters [3], which reflect the permeable and storage capacity of a reservoir and guide the engineers to choose rational development project. Permeability is the capacity for the porous medium to transmit fluid. And porosity refers to the ratio of pore volume to bulk volume. [5] To understand the permeability and porosity in the real production process and the high-permeable zone by long-term waterflooding, a customized macroscopic two-dimensional etched network channel model was used to conduct the experiment.

In 1856, Darcy observed the flow of water and did some research on the permeation. [6] He did experiment on water flowing through sand sample and analyzed the experiment result, showing as

$$Q = \frac{kA \Delta P}{\mu L} \quad (104.1)$$

where  $Q$  represents the rate of flow of water downward through the sand ( $\text{cm}^3/\text{s}$ ).  $A$  is the section area for the holder contained sand.  $\mu$  is the viscosity of the water ( $\text{m Pa/s}$ ), and  $\Delta P$  is the differential pressure ( $\text{atm}$ ).  $L$  stands for the length for the holder contains sand ( $\text{cm}$ ).

According to Darcy's law, the rate of the flow is related to permeability. However, there are also some assumptions for using Darcy's law—(1) there is no reaction between fluid and rock, (2) there is only one phase fluid, (3) a laminar and steady state flow.

Falling head and constant head are two basic methods to measure the permeability for different coefficients of permeability.

As a characteristic of rock, the absolute permeability is determined by measurements of the flow rate of a single fluid through the rock. However, relative permeability is a function of the rock and fluid chemical as well as physical properties. Methods to measure the two-phase relative permeability are well developed, and basically there are two methods to determine the relative permeability in laboratory: steady state methods and unsteady state methods [7, 8].

To determine relative permeability, steady state methods are the most reliable and widest applicable methods. And the saturation is measured directly because of the capillary equilibrium. At the same time, the calculation method is based on Darcy's law.

#### (a) Basic Principle

Steady state methods mean that to reach equilibrium, two or three fluids are injected simultaneously at constant rates or pressure for same durations. The saturations, flow rates, and pressure gradients are measured, and Darcy's law is used to calculate the effective permeability of each phase. In the end, a series data of relative permeability and saturation are obtained by changing the ratio of injection rates and repeating the measurement procedure when equilibrium is attained. The advantages of steady state methods are reliability, and they can be used to determine the relative permeability of a wide range of saturation. Basically, steady state methods include Hassler method (single-sample dynamic, stationary phase), Penn State, and modified Penn State [9] based on the different ways to reach capillary equilibrium between fluids.

#### (b) The Measurement Process [10]:

1. Vacuum the rock sample and saturate it with water, measure the absolute permeability;
2. Flood the rock sample with oil to irreducible water saturation, measure the effective permeability;
3. Keep the total flow rate fixed, inject water and oil at a fixed ratio. When the pressure and flow rate in the rock sample are stable and oil is distributed evenly in rock sample, record the pressure of inlet and outlet, flow rate of water and oil, measure the water saturation. Then, calculate the effective permeability and relative permeability of each phase by Darcy's law;
4. Change the injection ratio of water and oil, repeat the experiment, and a series of oil and water permeability at different water saturation can be got;
5. Draw the relative permeability curve (relative permeability versus saturation).

The capillary end effect is a phenomenon that the saturation of the wetting phase is higher close to the inlet and outlet ends of the rock samples caused by greater affinity of the wetting phase to remain in pore capillaries rather than to exit to a non-capillary

space. It has two features: (a) in a certain distance away from outlet, the wetting phase saturation is higher; (b) the time wetting phase flowing out is shortly delayed. There are methods to eliminate end effect:

**Hassler's Technique:** Place porous plates of the same wettability as the rock sample at both ends of the rock sample. The wetting phase has to pass through the fully saturated plates, where the non-wetting phase is flowed directly into the core.

**Penn State Method:** Place porous material which is in contact with the inlet and outlet of the core directly. All fluids flow through the porous material, which is the main difference with Hassler's technique.

Flood at a high flow so that the influence of capillary can be neglected compared with viscous forces. At the same time, longer cores were used for the experiment while restricting the pressure and saturation measurements to the inner sections of the cores. However, among all the methods, pressure drops of each phase cannot be measured separately.

## 104.2 Materials and Equipment

Fluids: kerosene (density 0.78 g/cm<sup>3</sup>, viscosity 0.8892 mPa s); DI water; dye.

Equipment: 1/8" flexible tubing; female luer to 1/8" house connection; 1/8" × 1/8" × 1/8" tee; bracket; connection; ball valves; graduated glass tubing; beaker; KDS Gemini 88 syringe pump; micromodel; analytical balance; graduate cylinder; stop watch; vacuum pump; pressure transmitter;

**Micromodel:** As for the customized macroscopic two-dimensional etched network channel model used in the experiment, the permeability was defined as the capacity for fluid flows through the pore etched on the model. Dyed water was conducted for the experiment to satisfied the assumption for Darcy's law. The pump KDS Gemini 88 syringe pump could supply a constant flow rate of the flow (Fig. 104.1).

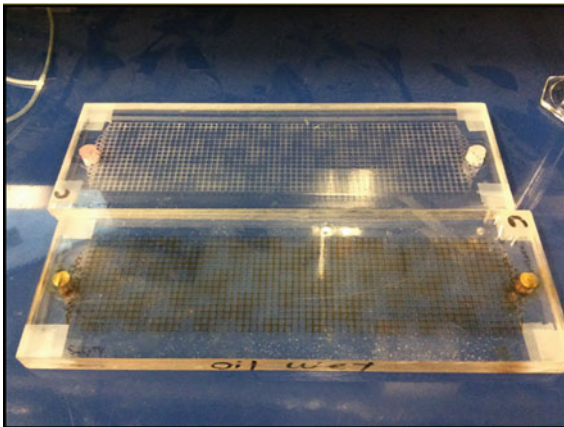


**Fig. 104.1.** 2D high-permeable model with etched network channels

### 104.3 Methodology

#### 104.3.1 Permeability Measurement

The experiment set up is shown in Figs. 104.2 and 104.3 for falling head and constant head, respectively.

For the falling head permeability test [11], connect the experiment set up as the designed.

1. Saturate the micromodel by dyed water with no bubble in micromodel.
2. Fill the graduated glass tubing with dyed water.
3. Open the valve and take pictures on the water surface in glass tubing at every 20 s.
4. Repeat the experiment for several times, start and stop record the time at the same height.
5. Pick the middle section of the tubing for recording with the consideration of effect of the inlet or outlet of the tubing into consideration.

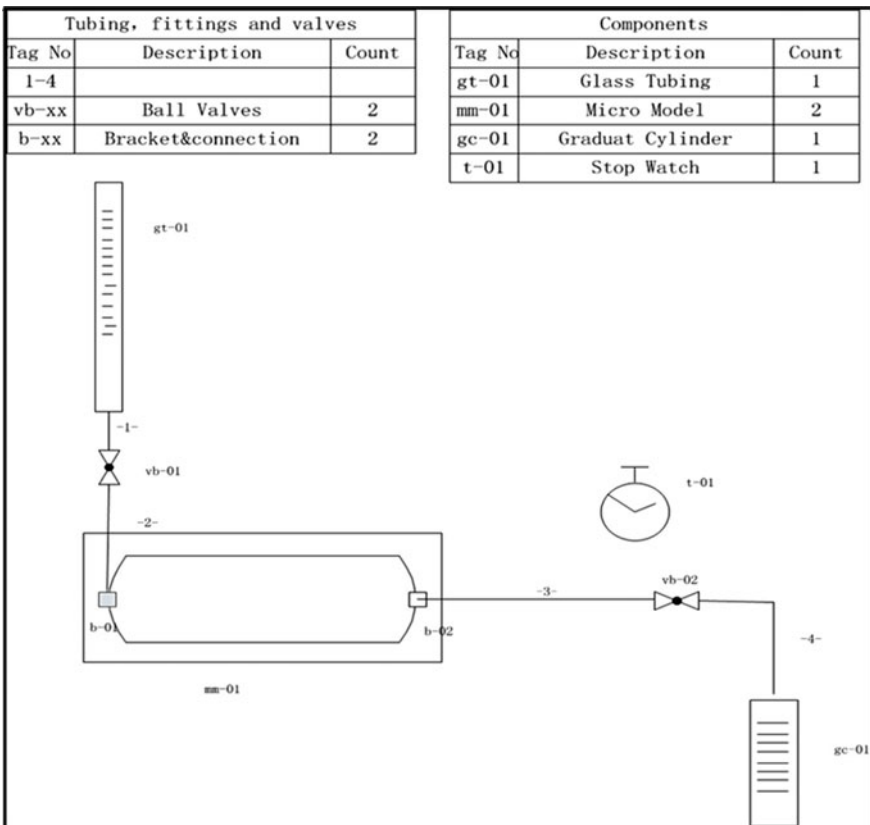
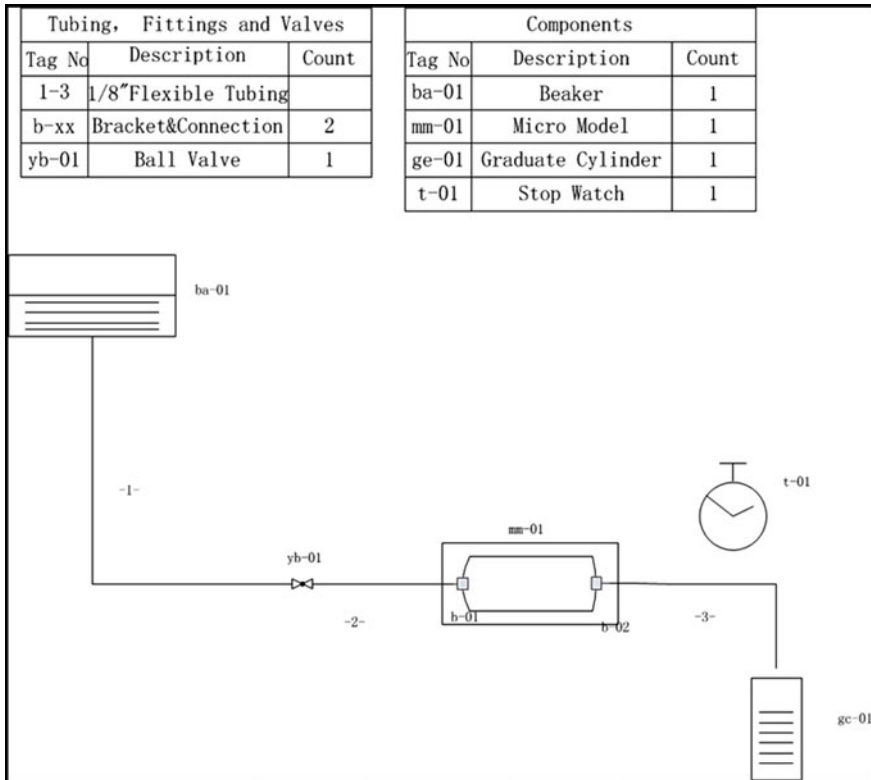


Fig. 104.2. Falling head permeability test apparatus



**Fig. 104.3.** Constant head permeability test apparatus

For the constant head permeability test, equivalently, connect the set up as designed.

1. Put the container on an appropriate height.
2. Use the graduated cylinder to collect the water flowing through the micromodel and also record the time.
3. Repeat the constant head test for three times and use the average value to calculate permeability.

### 104.3.2 Porosity Measurement

For porosity test, connect the set up as showed above.

1. Push the oil into the micromodel by syringe and start to record the time when oil reaches the etch area.
2. Stop time recording when oil leaves the etch area.
3. Using the time and rate of flow to calculate how much oil injected into the micromodel (Fig. 104.5).

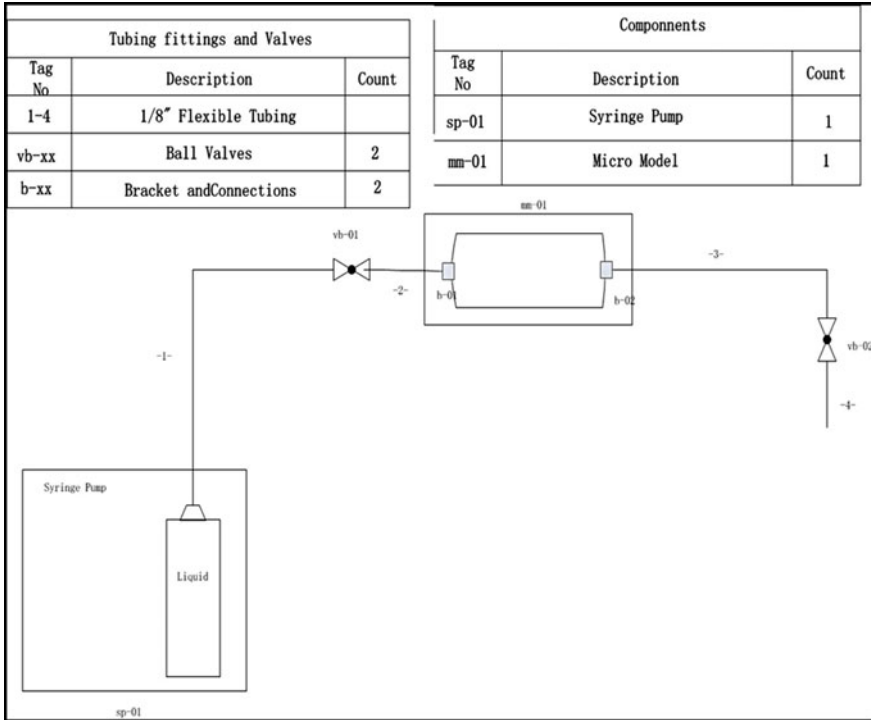


**Fig. 104.4.** Porosity test apparatus

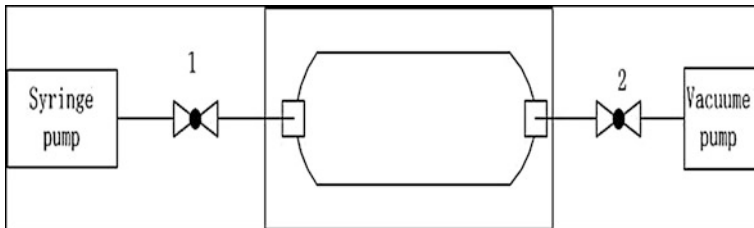


**Fig. 104.5.** Vacuum set up

### 104.3.3 Relative Permeability Measurement

For relative permeable test [12],

1. Use the vacuum pump to vacuum the micromodel and saturate it with dyed oil;
  - (a) Inject dyed oil to valve 1;
  - (b) Close valve 1 and valve 2;
  - (c) Connect the set up to vacuum pump;
  - (d) Open valve 2 and turn on vacuum pump, vacuum for 30 min;

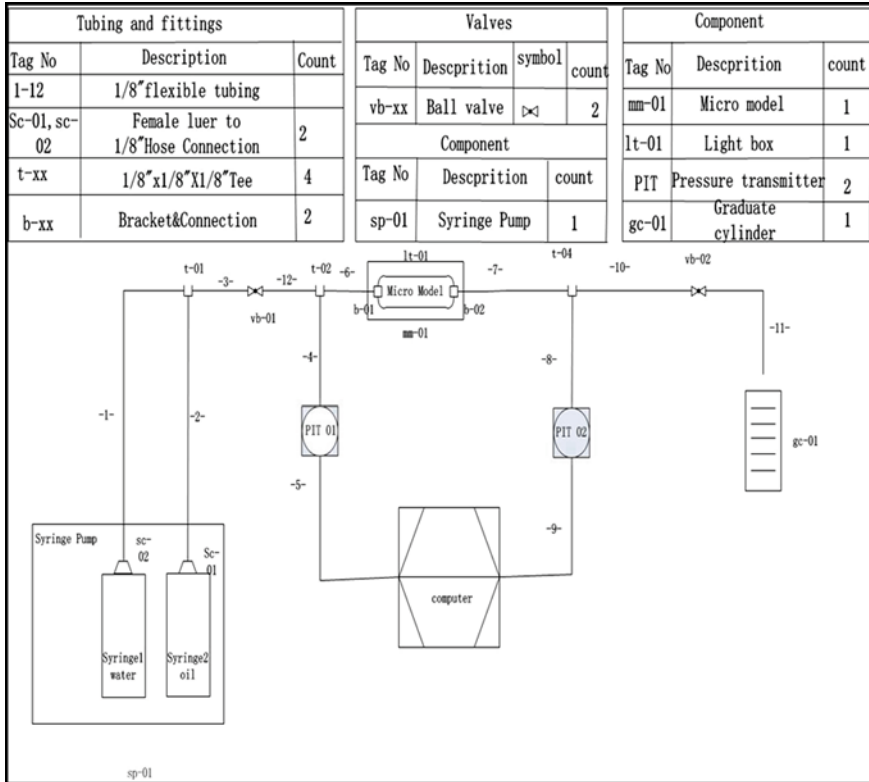


**Fig. 104.6.** Relative permeability test apparatus

- (e) Close valve 2 and turnoff vacuum pump;
- (f) Open valve 1.
2. Connect the experimental set up as Fig. 104.4 shows;
3. Keep the total flow rate fixed, set the flow rate of water and oil on syringe pump.
4. Wait for the water–oil interface to be stable and the pressure steady, record the pressure difference, the inject rate of oil and water, measure the total mass of the fluid flow out and total volume of the fluid.
5. Change the oil–water ratio (10:1, 5:1, 2:1, 1:1, 1:2, 1:5, 1:10) and repeat the experiment.

## 104.4 Results

### 104.4.1 Permeability Measurement with Falling Head

According to Darcy's law,

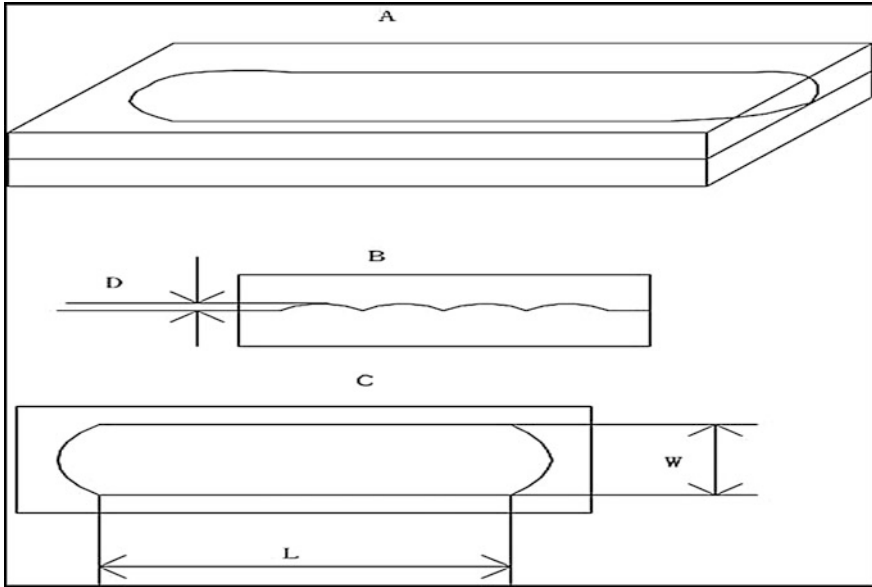


**Fig. 104.7.** Geometric characterization of the micromodel

$$Q = \frac{kA \Delta P}{\mu L} \quad (104.2)$$

where all the units are Darcy's unit.  $Q$  is the rate flow, ( $\text{cm}^3/\text{s}$ ).  $\mu$  is the fluid viscosity ( $\text{mPa s}$ ).  $L$  is the length of the etched area of micromodel ( $\text{cm}$ ).  $\Delta p$  is the differential pressure between inlet and outlet of micromodel ( $\text{atm}$ ).  $A$  is the section area of the fluid flow, which is the cross-sectional area of micromodel.

$$A = W \cdot D \quad (104.3)$$

where  $W$  is the width of the pore area and  $D$  is the etched depth.

In the falling head test,

$$\Delta p = \rho gh \quad (104.4)$$

$$Q = u \cdot a \quad (104.5)$$

where  $u$  is the rate of the water surface drop ( $\text{cm/s}$ ) and  $a$  is the cross-sectional area of the pipe ( $\text{cm}^2$ ).

Then the equation of Darcy's law could be changed into



$$ua = \frac{kA \rho gh}{\mu L} \quad (104.6)$$

Also,

$$u = -\frac{dh}{dt} \quad (104.7)$$

So,

$$-\frac{dh}{dt}a = \frac{kA \rho gh}{\mu L} \quad (104.8)$$

Then,

$$-\frac{1}{h}dh = \frac{kA \rho g}{\mu a L} dt \quad (104.9)$$

Integrate from position 1( $h_1, t_1$ ) to position 2( $h_2, t_2$ )

$$\int_{h_1}^{h_2} -\frac{1}{h} dh = \int_{t_1}^{t_2} \frac{kA \rho g}{\mu a L} dt \quad (104.10)$$

$$\ln \frac{h_1}{h_2} = kA \frac{\rho g}{\mu a L} (t_2 - t_1) \quad (104.11)$$

So, a linear relationship was obtained,

$$\ln \frac{h_1}{h_2} = k \frac{A \rho g}{\mu a L} (t_2 - t_1) \quad (104.12)$$

According to the equation, a linear relationship between  $\ln \frac{h_1}{h_2}$  and  $\frac{A \rho g}{\mu a L} (t_2 - t_1)$  was obtained, in which the height of the water ( $h$ ) and the time cost at different height ( $t$ ) were the two parameters recorded in the experiment. Taking into consideration that the flow may not be linear flow, when linear fitting, neglect the point that obviously do not conform to the linear pattern. And the gradient of the line is the permeability that gets from the falling head permeability test (Figs. 104.8, 104.9, and 104.10; Table 104.1).

The average of the permeability is **103.43 Darcy**.

#### 104.4.2 Permeability Measurement with Constant Head

In the constant head experiment, the pressure sensor was used to monitor the pressure difference. And the results are shown in Table 104.2.

The average of the permeability is **93.16 Darcy** (Table 104.3).

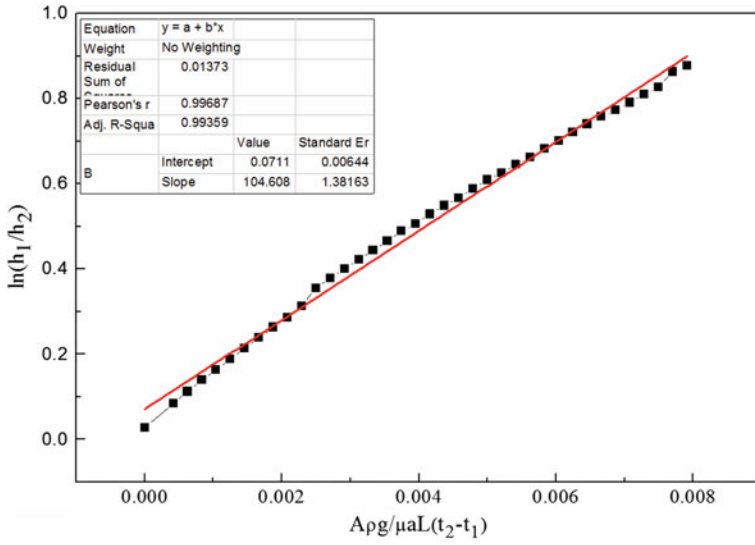


Fig. 104.8. Falling head permeability test 1

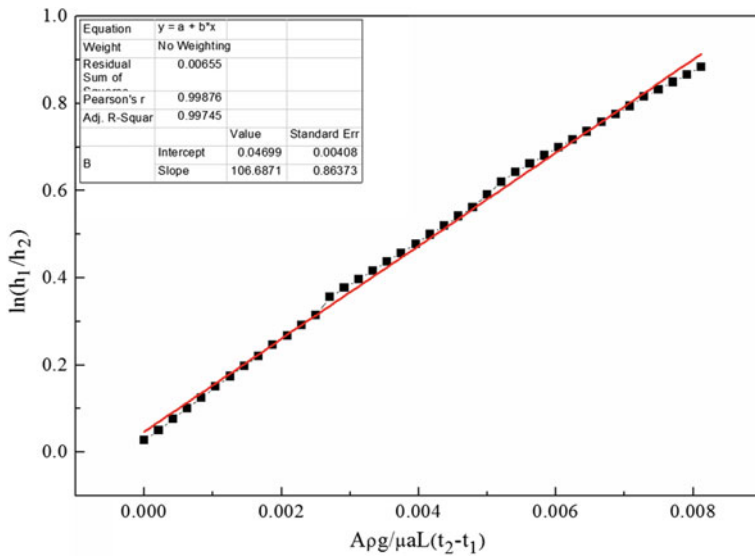
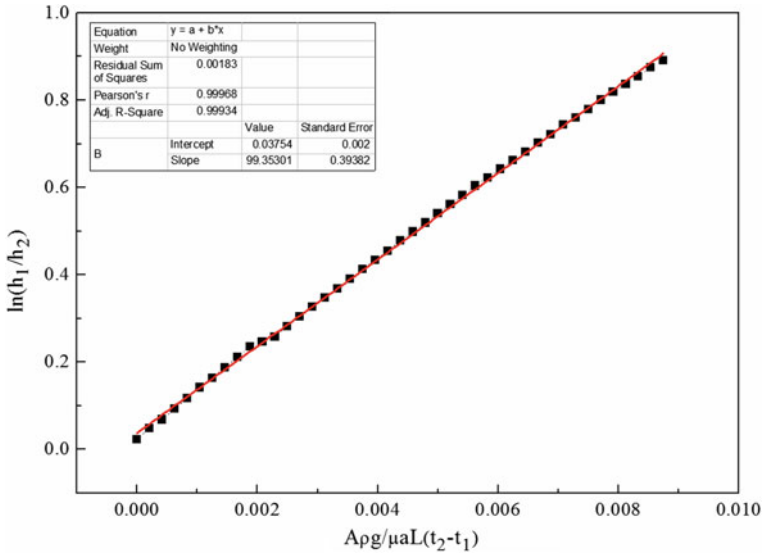


Fig. 104.9. Falling head permeability test 2



**Fig. 104.10.** Falling head permeability test 3

**Table 104.1.** Falling head permeability test

Attempt	1	2	3
K	104.25	106.69	99.35

**Table 104.2.** Contant head permeable test

Attempt	V (mL)	T (s)	Q (cm <sup>3</sup> /s)	P <sub>1</sub> (psi)	P <sub>2</sub> (psi)	Δp (psi)	K (Darcy)
1	5	1790	0.00279	14.788	14.660	0.00827	90.14
2	5	3000	0.00167	14.826	14.758	0.00468	95.16
3	5	2040	0.00245	14.803	14.703	0.00695	94.19

Comparing the two different method derived from Darcy’s equation which characterized the permeable and discussing the experimental results in details, the constant head method to characterize the permeability was more accurate.

**104.4.3 Porosity**

According to the definition of porosity,

$$\varphi = \frac{V_P}{V_B} \times 100\% \tag{104.13}$$

where  $V_B$  is the bulk volume and  $V_P$  is the pore volume.

**Table 104.3.** Relative permeable test

Ratio of oil and water	Oil inject rate (ml/min)	Water inject rate (ml/min)	$P_1$ (psi)	$P_2$ (psi)	Time (min)	Total volume (ml)	Mass (g)
Pure oil	0.1000	0	14.802	14.475	/	/	/
10:1	0.3640	0.0364	14.761	14.472	83.57	32.9	26.124
5:1	0.3330	0.0670	15.097	14.320	35.47	14.5	11.772
2:1	0.2670	0.1330	15.000	14.295	21.92	8.8	7.480
1:1	0.2000	0.2000	15.114	14.300	19.03	8.0	7.120
1:2	0.1330	0.2670	15.058	14.320	32.64	4.9	4.504
1:5	0.0670	0.3330	15.050	14.273	26.41	10.6	10.204
1:10	0.0364	0.3640	15.077	14.263	39.34	16.0	15.670

$$V_B = W \times L \times D \quad (104.14)$$

$$V_P = Q \times t \quad (104.15)$$

So the porosity could be calculated as

$$\varphi = 59.7\%$$

#### 104.4.4 Oil and Water Relative Permeability

The results and relative permeable curve are shown in Table 104.4 and Fig. 104.7.

Since the experiment was started when the micromodel was saturated with oil, the starting point of water saturation was zero rather than irreducible water saturation.

In the area A (Fig. 104.6), when water saturation increased, because of the impediment of oil, the permeability of water dropped sharply and the permeability of water increased slowly but steadily. The flow in the micromodel was getting stable gradually. When the water saturation reached a certain number, the flow ability of oil and water was the same. When it came to permeability curve, oil and water relative permeability curve cross (the cross point was called point, and the water saturation was called isotonic saturation). It was easily noticed that the isotonic saturation was more

**Table 104.4.** Porosity test

Attempt	$t$ (s)	$V_P$ (mL)
1	851.23	1.4187
2	914.75	1.5246
3	868.91	1.4482
Average		1.4683

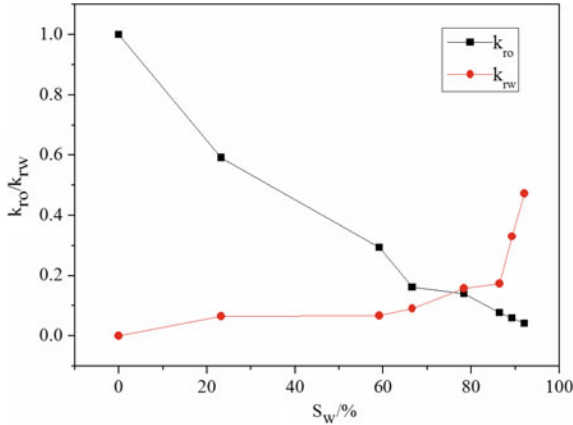


Fig. 104.11. Relative permeable curve

Table 104.5. Relative permeable measurement results

$k_o/D$	$k_{ro}$	$k_w/D$	$k_{rw}$	$S_W/\%$
100.5	1	0	0	0
59.5	0.592	6.7	0.066	23.2
29.5	0.294	6.8	0.067	59.1
16.3	0.162	9.14	0.091	66.6
14.1	0.14	15.8	0.158	78.4
7.8	0.077	17.5	0.174	86.4
5.9	0.059	33.2	0.330	89.3
4.2	0.042	47.5	0.473	92.1

than 50%, so the micromodel used in experiment was water wet. In the area C, the oil saturation dropped, getting close to zero and the water saturation rose phenomenally.

During the imbibition, the relative permeability of non-wetting phase was smaller than that during the drainage process. However, for wetting phase, the relative permeability during the imbibition was nearly the same as that during the drainage [13] (Fig. 104.11; Table 104.5).

$$K_o = \frac{Q_o \mu_o L}{A \Delta P} \tag{104.16}$$

$$K_{ro} = \frac{K_o}{K} \tag{104.17}$$

$$K_w = \frac{Q_w \mu_w L}{A \Delta P} \quad (104.18)$$

$$K_{rw} = \frac{K_w}{K} \quad (104.19)$$

## 104.5 Conclusion

1. The customized macroscopic two-dimensional etched network channel model could be used to simulate the high-permeable zone representatively.
2. Two different ways to measure the permeability of the model was conducted. The results indicated that the constant head method was more accurate for the high coefficient of permeability porous media.
3. To simulate the primitive formation condition, the kerosene was saturated with the model and the porosity was calculated after the pore fulfilled. The measurement result could define the model as high porosity.
4. The relative permeable curve was obtained from steady state method. From the diagram the isotonic saturation was more than 50%, so the micromodel used in experiment was water wet.

**Acknowledgements.** The work was supported by the National Science Fund for Distinguished Young Scholars (51425406), the Chang Jiang Scholars Program (T2014152), the National Science Fund (U1663206), the Climb Taishan Scholar Program in Shandong Province (tspd20161004), the Fundamental Research Funds for the Central Universities (15CX08003A).

## References

1. Khezrnejad A, James L, Johansen T (2015) Nanofluid enhanced oil recovery—mobility ratio, surface chemistry, or both?, In: International symposium of the Society of Core Analysts, St. John's Newfoundland and Labrador, Canada, pp 16–21
2. Han, H Dusseault MB, Ioannidis M, Xu B (2006) Multiscale pore structure characterization by combining image analysis and mercury porosimetry, In: SPE Europe/EAGE annual conference and exhibition, Society of Petroleum Engineers
3. Tiab D, Donaldson EC (2015) Petrophysics: theory and practice of measuring reservoir rock and fluid transport properties. Gulf professional publishing, Houston, Texas
4. Fulin Z (2000) Oilfield chemistry. China University of Petroleum Press, Dongying, Shandong, China, 148
5. Craft BC, Hawkins MF (1960) Applied petroleum reservoir engineering, In: JSTOR
6. Amyx JW, Bass DM, Whiting RL (1960) Petroleum reservoir engineering: physical properties. McGraw-Hill College, New York
7. Honarpour M, Mahmood S (1988) Relative-permeability measurements: An overview. J Petrol Technol 40:963–966

8. Alemán MA, Ramamohan TR, Slattery JC (1989) The difference between steady-state and unsteady-state relative permeabilities. *Transp Porous Media* 4:449–493
9. Honarpour MM, Koederitz F, Herbert A (1986) *Relative permeability of petroleum reservoirs*. CRC Press, Boca Raton, FL
10. Jishun Q, Aifen L, Renyuan S (2001) *Reservoir physics*. Petroleum University Publishing House, Dongying, pp 77–78
11. Fwa T, Tan S, Chuai C (1998) Permeability measurement of base materials using falling-head test apparatus. *Transp Res Record J Transp Res Board* 1615(1):94–99
12. Osoba J, Richardson J, Kerver J, Hafford J, Blair P (1951) Laboratory measurements of relative permeability. *J Petrol Technol* 3:47–56
13. Bennion DB, Bachu S (2010) Drainage and imbibition CO<sub>2</sub>/brine relative permeability curves at reservoir conditions for high-permeability carbonate rocks, In: SPE annual technical conference and exhibition, society of petroleum engineers